



## NRC Publications Archive Archives des publications du CNRC

### Room Temperature Ionic Liquid Electrolytes Based on Azepanium Imide Salts for Lithium Batteries

Salem, Nuha; Nicodemou, Lucas; Abu-Lebdeh, Yaser; Davidson, Isobel J.

This publication could be one of several versions: author's original, accepted manuscript or the publisher's version. /  
La version de cette publication peut être l'une des suivantes : la version prépublication de l'auteur, la version  
acceptée du manuscrit ou la version de l'éditeur.

For the publisher's version, please access the DOI link below. / Pour consulter la version de l'éditeur, utilisez le lien  
DOI ci-dessous.

#### **Publisher's version / Version de l'éditeur:**

<https://doi.org/10.1149/2.102202jes>

*Journal of The Electrochemical Society*, 59, 2, pp. A172-A176, 2011-12-22

#### **NRC Publications Record / Notice d'Archives des publications de CNRC:**

<https://nrc-publications.canada.ca/eng/view/object/?id=96c59f10-ae85-48aa-a448-063089799260>

<https://publications-cnrc.canada.ca/fra/voir/objet/?id=96c59f10-ae85-48aa-a448-063089799260>

Access and use of this website and the material on it are subject to the Terms and Conditions set forth at

<https://nrc-publications.canada.ca/eng/copyright>

READ THESE TERMS AND CONDITIONS CAREFULLY BEFORE USING THIS WEBSITE.

L'accès à ce site Web et l'utilisation de son contenu sont assujettis aux conditions présentées dans le site

<https://publications-cnrc.canada.ca/fra/droits>

LISEZ CES CONDITIONS ATTENTIVEMENT AVANT D'UTILISER CE SITE WEB.

#### **Questions?** Contact the NRC Publications Archive team at

PublicationsArchive-ArchivesPublications@nrc-cnrc.gc.ca. If you wish to email the authors directly, please see the  
first page of the publication for their contact information.

**Vous avez des questions?** Nous pouvons vous aider. Pour communiquer directement avec un auteur, consultez la  
première page de la revue dans laquelle son article a été publié afin de trouver ses coordonnées. Si vous n'arrivez  
pas à les repérer, communiquez avec nous à PublicationsArchive-ArchivesPublications@nrc-cnrc.gc.ca.





## Room Temperature Ionic Liquid Electrolytes Based on Azepanium Imide Salts for Lithium Batteries

Nuha Salem, Lucas Nicodemou, Yaser Abu-Lebdeh,<sup>\*,z</sup> and Isobel J. Davidson

Institute for Chemical Process and Environmental Technology, National Research Council Canada, Ottawa, Ontario K1A 0R6, Canada

Ionic liquids based on the imide salts of the dialkyl azepanium cation, AZ ( $R_1, R_2$ ) were synthesized, characterized, and evaluated as electrolytes in lithium batteries. Nine salts were synthesized with variation in the length of the two alkyl groups [ $R_1, R_2$  = methyl (1), ethyl (2), propyl (3) and butyl (4)]. It was found that the asymmetric ones with  $R_2 - R_1 \geq 2$  are liquids at ambient temperature. The three room-temperature ionic liquids (AZ13-TFSI, AZ14-TFSI, AZ24-TFSI) showed, in the neat form, ionic conductivities in the range of 0.1–0.6 mS/cm, viscosities of 260–350 cP and an electrochemical window of 5.5–6 V. It was found that mixing the ionic liquids with ethylene carbonate gave electrolytes with lower viscosities, increased conductivities and improved electrochemical cathodic stability. Electrolytes based on the ILs were evaluated in lithium half cells with different chemistries; Li/LiFePO<sub>4</sub>, Li/Li<sub>4</sub>Ti<sub>5</sub>O<sub>12</sub>, Li/LiCoO<sub>2</sub>; and in the case of AZ14-TFSI a Li/LiFePO<sub>4</sub> cell, gave discharge capacities reaching 125 mAh.g<sup>-1</sup> over 100 cycles with 98% coulombic efficiencies.

© 2011 The Electrochemical Society. [DOI: 10.1149/2.102202jes] All rights reserved.

Manuscript submitted August 17, 2011; revised manuscript received October 25, 2011. Published December 22, 2011. This was Paper 393 presented at the Montreal, QC, Canada, Meeting of the Society, May 1–6, 2011.

Li-ion batteries have proven to be very successful in portable consumer electronics mainly due to their high energy density and long cycle life. This has made them a very viable candidate for use in a more energy-demanding applications such as electric vehicles (EV, HEV, PHEV) and large energy storage systems for the electrical grid.<sup>1–4</sup> There is a huge interest in developing new and improved materials for Li-ion batteries to enhance their performance, safety and lower their cost. One of the main components of the battery is the electrolyte which is composed currently of a lithium salt (LiPF<sub>6</sub>) dissolved in a mixture of aprotic (carbonate) molecular solvents.<sup>5</sup> Solvents such as ethylene carbonate (EC) or dimethyl carbonate (DMC) are both flammable and volatile and can undergo undesired (exothermic) reactions while in contact with other battery components causing a major safety concern.<sup>6</sup> In the last decade, ionic liquids, ILs, have been investigated as an alternative electrolyte system due to their excellent thermal and physiochemical properties such as non-flammability, negligible vapor pressure, good dissolution power, good electrochemical stability, wide liquid range and intrinsic ionic conductivity.<sup>6–12</sup> A wide variety of salt (cation and anion) chemistry have been investigated in order to enable their successful operation in lithium and lithium-ion batteries which turned out to be a big challenge due to poor cathodic stability, very high viscosity, compatibility with other active and inactive battery components, impurities and high cost.

Ionic liquids based on the ringed ammonium cations have been investigated extensively due to their enhanced cathodic stability among other things. From our previous work with spiro-ammonium imide salts we found that the melting points are higher than room temperature (>100°C)<sup>13</sup> which decreased as the size of one or both of the rings of the cation became large with the seven-membered ring showing the lowest melting points. This was due to the increased molecular disorder due to the presence of a high number of conformers leading to low entropy of crystallization and increased constrain on molecular packing. It has also been shown that uni-ringed ammonium salts tend to have lower melting points than the bi-ringed (spiro) ammoniums. There has been extensive research into the uni-ringed five-membered “pyrrolidinium” and six-membered “piperidinium” ILs due to the exceptional cathodic stability such as P13, P14, PP13 and PP14.<sup>14–19</sup> This work was undertaken as there are virtually no studies on the behavior of ionic liquids based on the seven-membered ring and their potential use in lithium batteries. During the course of the study, Belhocine et al published their work on similar ionic liquids but with no report of their battery performance.<sup>20,21</sup> Herein, we describe the

physical and chemical properties of synthesized azepanium imide salts and compare it with their five and six-membered counterparts and report on their potential use in lithium batteries.

### Experimental

**Synthesis of symmetric azepanium imide salts AZ ( $R_1 = R_2$ )-TFSI.**—Symmetric azepanium salts were prepared by single alkylation followed by ion exchange. All of the reactants used were analytical grade. First, 0.1 mol Hexamethyleneimine was dissolved in 100 mL of 1 M NaOH solution. This solution was stirred and heated using an oil bath until it began to reflux. Once the reaction mixture began to reflux, 0.1 mol of the desired alkyl bromide was added drop wise over a period of 30 minutes. The reaction mixture was removed from the heat, shielded from light and allowed to cool. 50 mL of cooled 10 M NaOH solution was then added to the reaction mixture and left for 2 hours. During this time the reaction mixture remained shielded from light. The azepanium bromide was isolated by vacuum filtration of the reaction mixture. The crystals were then dissolved in water. An equimolar amount of LiTFSI was also dissolved in water and the 2 solutions were combined in a round bottom flask and left until the oil layer separated completely. Finally, the azepanium salt was extracted and washed several times with distilled water and placed in the vacuum oven over night to dry.

**Synthesis of asymmetric azepanium imide salts AZ ( $R_1 \neq R_2$ )-TFSI.**—Asymmetric azepanium salts were prepared by two alkylation steps followed by ion exchange. Equimolar amounts of hexamethyleneimine and the bromoalkane of the longer alkyl chain (0.1 mol) were allowed to react in acetonitrile for 2 hours at 0°C and for overnight at room temperature. Solvent was removed under vacuum and the solid product was washed with ethyl ether several times then dried in vacuum oven. The white solid product was then dissolved in 1 M NaOH solution and the shorter bromoalkane was added drop wise at room temperature first then heated to 80°C for few hours. The reaction mixture was cooled to room temperature before more NaOH was added to precipitate the resulting azepanium bromide salt. The salt was then washed several times with diethyl ether, dried in vacuum oven and exchanged with an equimolar amount of LiTFSI in water. The resulting oil was separated from the aqueous layer with the help of dichloromethane, washed with water until no halide is present (tested using AgNO<sub>3</sub>) and filtered through activated alumina. Traces of water and CH<sub>2</sub>Cl<sub>2</sub> were removed using rotovap and the oil was dried in vacuum oven overnight before characterization.

\* Electrochemical Society Active Member.

<sup>z</sup> E-mail: Yaser.Abu-Lebdeh@nrc.gc.ca

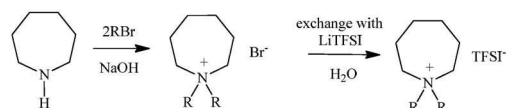
**Characterization.**— Proton NMR spectra were recorded using an oxford 400 run at 400 Mhz in  $\text{CDCl}_3$ . For AZ14: (3H,  $\delta$ 0.97, t), (2H,  $\delta$ 1.40, six), (6H,  $\delta$ 1.72, t), (4H,  $\delta$ 1.87, s), (3H,  $\delta$ 2.97, s), (2H,  $\delta$ 3.21, m), (4H,  $\delta$ 3.30, m). AZ13: (3H,  $\delta$ 1.01, t), (6H,  $\delta$ 1.78, m), (4H,  $\delta$ 1.88, s), (3H,  $\delta$ 3.00, s), (2H,  $\delta$ 3.21, m), (4H,  $\delta$ 3.41, m). AZ12: (3H,  $\delta$ 1.41, t), (4H,  $\delta$ 1.71, m), (4H,  $\delta$ 1.89, s), (3H,  $\delta$ 3.00, s), (6H,  $\delta$ 3.38, m). AZ24: (3H,  $\delta$ 0.93, t), (3H,  $\delta$ 1.27, t), (2H,  $\delta$ 1.34, six), (6H,  $\delta$ 1.61, m), (4H,  $\delta$ 1.84, s), (2H,  $\delta$ 3.12, m), (6H,  $\delta$ 3.30, m). AZ23: (3H,  $\delta$ 1.03, t), (3H,  $\delta$ 1.34, t), (6H,  $\delta$ 1.73, m), (4H,  $\delta$ 1.90, s), (2H,  $\delta$ 3.14, m), (6H,  $\delta$ 3.36, m). AZ22: (6H,  $\delta$ 1.30, t), (4H,  $\delta$ 1.68, quin), (4H,  $\delta$ 1.86, s), (8H,  $\delta$ 3.29, m). AZ33: (6H,  $\delta$ 1.01, t), (8H,  $\delta$ 1.71, m), (4H,  $\delta$ 1.90, s), (4H,  $\delta$ 3.16, m), (4H,  $\delta$ 3.39, m). AZ11: (4H,  $\delta$ 1.63, (4H,  $\delta$ 1.80, s), (6H,  $\delta$ -3.00, s), (4H,  $\delta$ -3.35, m)

DSC analysis was recorded using a TA instruments 2920 modulated DSC. All samples were sealed in aluminum pans inside an Ar-filled glove box and then scanned from  $-150$  to  $100^\circ\text{C}$  at a rate of  $5^\circ\text{C min}^{-1}$  under helium gas. Viscosity measurements were recorded using a CANNON viscometer No. 200 and a Brookfield DV-I+ viscometer. Measurements were recorded at intervals of  $10^\circ\text{C}$  from  $-5$  to  $80^\circ\text{C}$ . Conductivity measurements were performed using the AC impedance spectroscopy technique where the electrolyte solutions were poured into a two-platinum-electrode conductivity cell with a cell constant of  $1\text{ cm}^{-1}$ . The frequency was swept between  $1\text{ kHz}$  and  $1\text{ Hz}$  using Princeton Applied Research PAR 263A potentiostat coupled with a Solartron frequency response analyzer FRA 1255B. The temperature was varied between  $-20$  and  $80^\circ\text{C}$  allowing  $20\text{ min}$  for thermal equilibration. Linear sweep voltammograms were conducted using a platinum microelectrode ( $25\text{ }\mu\text{m}$ ) and a silver wire as a counter and reference electrode. These measurements were done using Princeton Applied Research PAR 263A potentiostat at room temperature with a scan rate of  $10\text{ mV s}^{-1}$ . Battery investigations were carried out with coin-type cells. Cathode material was made from a slurry containing 75% active material, 7.5% KS-4 graphite, 7.5% Super-S carbon and 10% PVDF binder dissolved in NMP, all by weight. The slurry was casted onto an aluminum foil and dried overnight at  $80^\circ\text{C}$  in a vacuum oven. Electrode disks of  $12.7\text{ mm}$  diameter were punched from the coated foil and pressed at  $0.5\text{ ton}$  pressure. The cells were assembled in an Ar-filled dry box at room temperature using Li as anode and 2 layers of microporous polypropylene separators (Celgard 3501). Cell performance was evaluated by galvanostatic experiments carried out on a multichannel Arbin battery cycler. Li/LiFePO<sub>4</sub> and Li/LiCoO<sub>2</sub> were cycled at a potential range  $2.5\text{--}4.2\text{ V}$  and Li/Li<sub>4</sub>Ti<sub>5</sub>O<sub>12</sub> at  $1\text{--}2.2\text{ V}$ . The cells were charged and discharged at constant current density ( $\text{C}/12$ ) at  $20^\circ\text{C}$ .

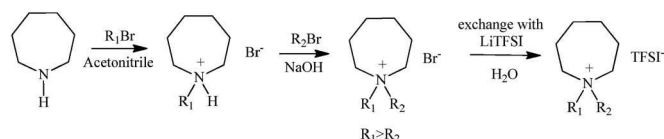
## Results and Discussion

**Synthesis and characterization of the azepanium imide salts.**— Scheme 1 describes the general synthetic procedure of the salts. We have adopted two methods; one for the symmetric salts based on “one-pot” direct double alkylation of the azepane with the corresponding

### Symmetric



### Asymmetric



**Scheme 1.** A schematic of the synthetic procedure for the azepanium imide salts.

**Table I.** DSC data for the nine prepared azepanium imide salts.

Asymmetric	Symmetric	Melting Point ( $^\circ\text{C}$ )	Glass Transition ( $^\circ\text{C}$ )	Freezing Point ( $^\circ\text{C}$ )
AZ14-TFSI			$-63.3$	
AZ13-TFSI		$15.5$	$-79.4$	$-37.4/-17.9$
AZ24-TFSI		$23.3$	$-82.3$	$-34.6/-4.1$
AZ12-TFSI		$50.7$		
AZ23-TFSI		$57.5$		
AZ34-TFSI		$62.0$		
	AZ11-TFSI	$72.1$		
	AZ22-TFSI	$89.8$		
	AZ33-TFSI	$97.9$		

alkyl bromide followed by exchange with LiTFSI. The other was more rigorous and a step-wise alkylation in order to lower the amount of impurities that might arise from the different possible compounds that can be formed. Azepane was alkylated first with the longer alkyl group using the corresponding alkyl bromide in acetonitrile followed by a second alkylation with the shorter one using the more reactive alkyl bromide, followed by exchange with LiTFSI. Nine salts were synthesized in total with good yields and purity as evidenced by  $^1\text{H}$  NMR. All salts were white solids except AZ14-TFSI, AZ13-TFSI and AZ24-TFSI which were liquids with clear to slightly yellowish color. A water content of  $14\text{ ppm}$  in AZ14-TFSI was obtained using Karl Fischer analysis.

**Differential scanning calorimetry.**— DSC scans of all synthesized salts were recorded and the melting and glass transition temperatures are summarized in Table I. It can be seen that the melting point of all the symmetric salts were above room temperature and decreased as the alkyl groups become shorter: AZ33-TFSI > AZ22-TFSI > AZ11-TFSI. When  $\text{R}_1$  and  $\text{R}_2$  were varied by one methylene group ( $\text{R}_2 - \text{R}_1 = 1$ ) the melting point dropped even further with the shortest alkyl groups showing the lowest temperature at  $50.7^\circ\text{C}$ : AZ34-TFSI > AZ23-TFSI > AZ12-TFSI. Further variation to two or more methylene groups ( $\text{R}_2 - \text{R}_1 = 2$ ) gave liquids at ambient temperature with melting points below  $25^\circ\text{C}$  such as AZ13-TFSI and AZ24-TFSI or showed no melting at all such as AZ14-TFSI, as shown in the heating scans in Figure 1. In general, this illustrates the profound effect of the size and shape of the cation on the crystallization behavior of the salt; it can be seen that asymmetric and longer aliphatic cations lead

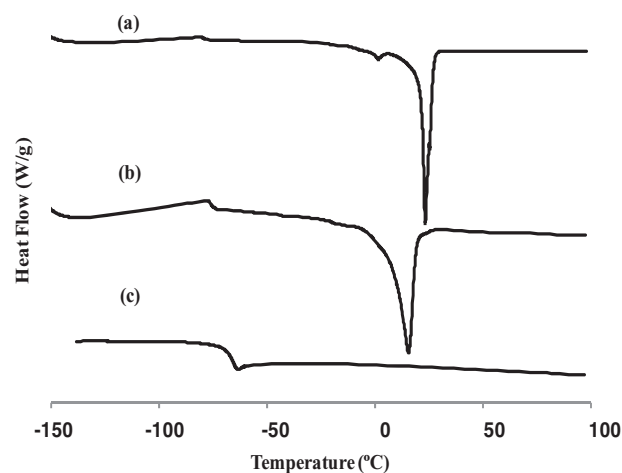


**Figure 1.** DSC of ionic liquids AZ24-TFSI (a), AZ13-TFSI (b) and AZ14-TFSI (c).

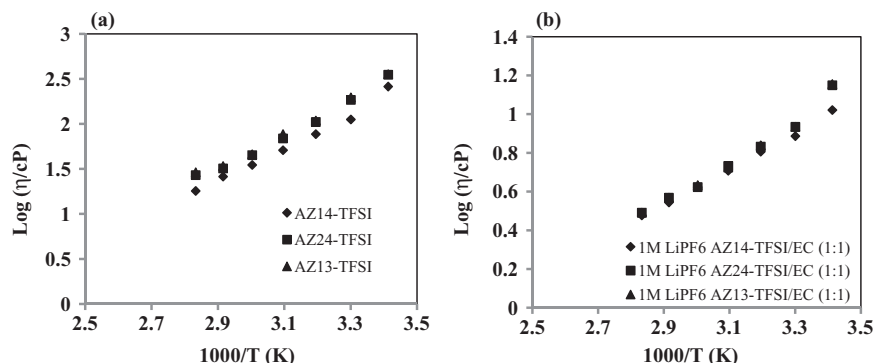


**Figure 2.** Viscosity as a function of temperature of neat AZ14-TFSI, AZ13-TFSI and AZ24-TFSI (a) and 1M LiPF<sub>6</sub> in IL: EC (1:1) electrolytes (b).

to lower melting points as the result of a more constrained molecular packing.<sup>15</sup> Also, the scan shows that the three ILs have a low glass transition temperature below  $-60^{\circ}\text{C}$  and increases in the order of AZ24-TFSI > AZ13-TFSI > AZ14-TFSI, that is indicative of the great molecular disorder present in these salts.<sup>15</sup> We also observed, data not shown here, that some of the symmetric salts showed an extra peak below melting that can be attributed to a solid-solid transition corresponding to a regular crystalline to plastic crystalline phase. A full study of this behavior will be discussed elsewhere.

**Viscosity and conductivity.**— Figure 2 shows the measured viscosities of the neat ionic liquids and their electrolytes. The viscosity of the neat AZ14-TFSI, AZ13-TFSI and AZ24-TFSI were measured at  $20^{\circ}\text{C}$  and found to be 260, 356 and 352 cP respectively. It can be seen from Figure 2a that the viscosities of all ionic liquids were inversely proportional to temperature within the range from 20 to  $80^{\circ}\text{C}$  reaching 18, 29, 27 cP respectively. When Ethylene carbonate, EC, was added at a 1:1 ratio along with LiPF<sub>6</sub> (1 M), the viscosities decreased significantly to values, at  $20^{\circ}\text{C}$ , of 10.5, 14.3 and 14.1 cP for AZ14-TFSI, AZ13-TFSI and AZ24-TFSI salts respectively, as shown in Figure 2b. The viscosity of ionic liquids is known to depend, among other things, on the molecular frictional forces that are governed by their size. It is known that bulky molecules show higher friction along with slow diffusion and therefore lead to higher viscosity. This explains the trend in the increase of viscosity of the dialkyl-ringed ammonium ionic liquids as the ring becomes bigger (260 cP: AZ14-TFSI > 182 cP: PP14-TFSI > 76 cP: P14-TFSI or 356 cP: AZ13-TFSI > 117 cP: PP13-TFSI > 63 cP: P13-TFSI.<sup>22</sup> Another factor that might contribute to this effect is the electrostatic interaction between the cation and the anion and their agglomeration into less-mobile, higher charge carriers. In the case of azepanium imide salts, these interactions are the weakest between one molecule of cation and anion due to the shielding effect of the bulky azepanium ring and the alkyl groups on the positive charge besides the delocalized negative charge of the imide anion, but it seems that this effect is counter balanced by the possible formation of ionic connected matrices of low mobility.<sup>15</sup>

Upon the addition of the LiPF<sub>6</sub> to a mixture of the ionic liquid and EC, the drop in bulk viscosity of the three ionic liquids can be attributed to the diluting effect of EC, due to its low viscosity (1.92 cP at  $40^{\circ}\text{C}$ ) and also its high dielectric constant of 89, that allows for greater solvation for lithium ions and for the ionic liquid molecules to become more mobile hence less viscous. In both figures, the viscosity showed the typical inverse linear relationship with temperature.

The ionic conductivities of the neat ionic liquids and its mixtures with EC were measured over a temperature range from  $-20$  to  $100^{\circ}\text{C}$  and are shown in Figures 3a and 3b. At  $20^{\circ}\text{C}$  the conductivities of AZ14-TFSI, AZ13-TFSI and AZ24-TFSI were found to be 0.61, 0.556 and  $0.104\text{ mS cm}^{-1}$ . The conductivity of the AZ14-TFSI is in good agreement with the value reported by Belhocine et al ( $0.59\text{ mS cm}^{-1}$ ).<sup>20</sup> It was also found that the conductivity increased as a function of temperature throughout the range from  $-20^{\circ}\text{C}$  to  $100^{\circ}\text{C}$  reaching 10.7, 13.0,  $10.0\text{ mS cm}^{-1}$ , respectively. The conductivity-temperature curves of the AZ13-TFSI and AZ24-TFSI showed discontinuities with large drops in the conductivity due to the freezing of the ionic liquids at the corresponding temperatures,  $13^{\circ}\text{C}$  for AZ13-TFSI and  $22^{\circ}\text{C}$  for AZ24-TFSI. The measured ionic conductivities of the seven-membered (azepanium) ILs are lower than the ones reported for the ionic liquid of the six-membered (piperidinium) and five-membered cations (pyrrolidinium) with the same alkyl groups (13 or 14) due to the large increase in viscosity as discussed earlier. An electrolyte solution was prepared by adding ethylene carbonate at a 1:1 weight ratio and LiPF<sub>6</sub> (1M) to AZ14-TFSI, AZ13-TFSI and AZ24-TFSI giving conductivities at  $20^{\circ}\text{C}$  of 5.88, 6.67,  $5.26\text{ mS cm}^{-1}$  respectively. This one-order of magnitude higher conductivities than the neat ILs is mainly due to the lower viscosities of the electrolyte solutions due to EC.

**Linear sweep voltammetry.**— The electrochemical stability of the ILs was evaluated using linear sweep voltammetry and the results are shown in Figure 4. The anodic voltammetry sweeps of the neat ionic liquids AZ14-TFSI, AZ13-TFSI and AZ24-TFSI showed an oxidation onset at 6.5 V, 6.0 V and 6.2 V (vs Li/Li<sup>+</sup>) respectively while

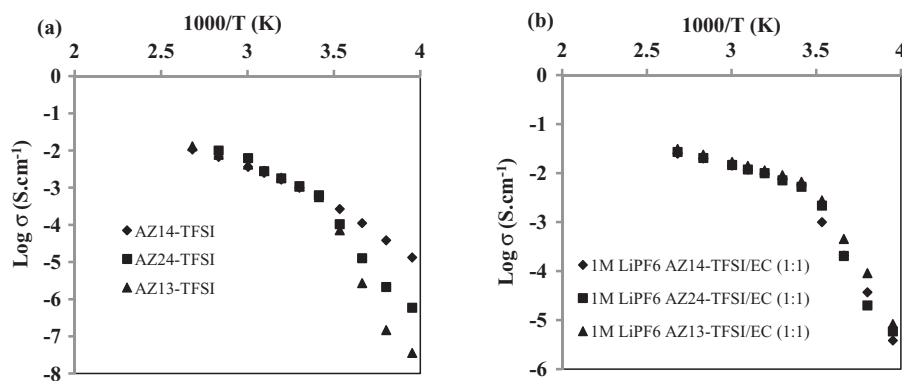


**Figure 3.** Conductivity as a function of temperature of neat AZ14-TFSI, AZ13-TFSI and AZ24-TFSI ionic liquids (a) and 1M LiPF<sub>6</sub> in IL:EC (1:1) electrolytes (b).



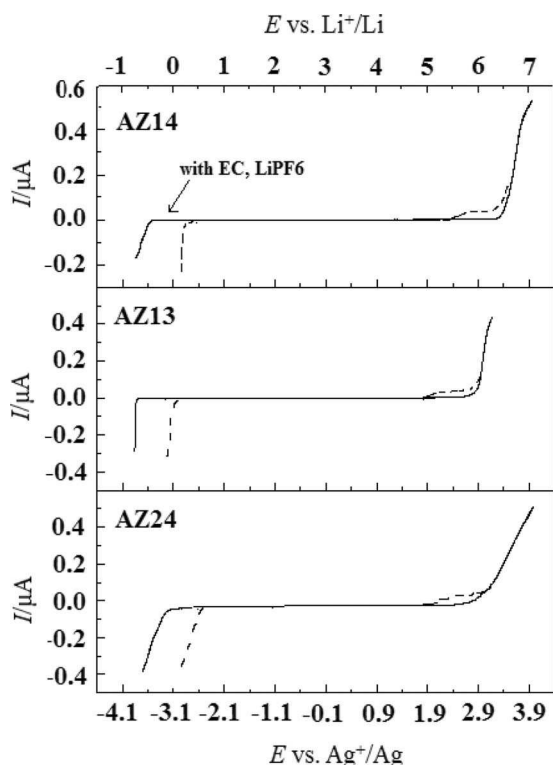


**Figure 4.** Linear sweep voltammetry of AZ14-TFSI, AZ13-TFSI and AZ24-TFSI using Pt working electrode and Ag wire reference electrode. Scan rate of  $10 \text{ mV s}^{-1}$ .

cathodic voltammetry sweeps of the same neat ionic liquids show an onset of reduction at 0.25 V, 0 V and 0.45 V. These values correspond to an electrochemical stability window of 6.25 V for AZ14-TFSI, 6.0 V for AZ13-TFSI, and 5.75 V for AZ24-TFSI. Belhocine et al found that AZ14-TFSI has similar potential window of 6.5 V with a slightly different oxidation onset at 6.25 V and different reduction onset at  $-0.25 \text{ V}$ , that is a higher cathodic stability and lower anodic stability compared to our AZ14-TFSI.<sup>20</sup> This could simply be attributed to a shift in potential due to the use of different electrodes and possibly the presence of impurities due to different synthetic methods.

Montanino et al have recently studied the effect of the cation aliphatic side chain length on the chemical and physicochemical properties of PP-TFSI ILs. With respect to the cathodic stability, it was proposed that the longer side chain although shields the positive charge and renders the cation to be kinetically stable its counter radical cations produced by reduction are more stable and therefore renders the cation thermodynamically less stable. This explains slightly the lower cathodic stability of the butyl substituent (AZ14-TFSI and AZ24-TFSI), and to a larger extent the lower cathodic stability of the seven-membered cations versus the five- and six-membered ones. It seems that the effect of the stability of the radical cation dominates over the shielding effect. Also, it has been suggested recently that the TFSI anion could play a previously overlooked role of limiting the cation stability due to possible cathodic (reduction) decomposition of the imide anion.<sup>23</sup>

Upon the addition of EC at 1:1 weight ratio and 1 M LiPF<sub>6</sub>, the cathodic stability improved for AZ14-TFSI by 1 V and for AZ13-TFSI and AZ24-TFSI by 0.75 V. This is the result of the passivation of the reduction product of mainly EC and PF<sub>6</sub> or TFSI anions. It is widely accepted now that the role of the cyclic carbonates versus linear ones or other solvents is dominant during the formation of the SEI in the initial battery cycling. EC in particular was found to be the main contributor to the SEI due to its high polarity and hence high solvation power.<sup>24</sup> In this case, the majority of lithium ion is surrounded by EC molecules causing them to accumulate at the electrode surface prior

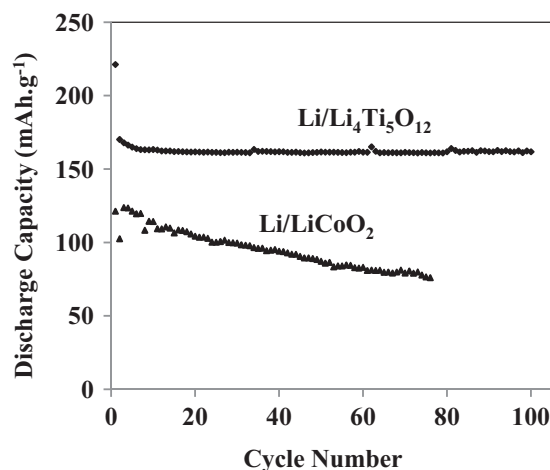


**Figure 5.** Cycling performance of Li/Li<sub>4</sub>Ti<sub>5</sub>O<sub>12</sub> and Li/LiCoO<sub>2</sub> half cell batteries using 1M LiPF<sub>6</sub> AZ14-TFSI/EC (1:1) wt/wt electrolyte.

to the intercalation/deintercalation process. This, along with other superior properties made the case for the choice of EC as a co-solvent.

**Battery performance.**— As discussed in the previous sections, the neat azeponium ionic liquids could not be evaluated as lithium battery electrolytes without the use of an additive or a co-solvent. Moreover, electrolytes based on AZ14-TFSI and LiTFSI were very viscous to handle and fabricate any batteries with. Therefore, electrolytes based on AZ14-TFSI and EC were formulated in the typical 1:1 ratio using LiPF<sub>6</sub> as the salt. Figure 5 shows the cycling performance of Li/Li<sub>4</sub>Ti<sub>5</sub>O<sub>12</sub> and Li/LiCoO<sub>2</sub> half cell batteries using this electrolyte. The Li/Li<sub>4</sub>Ti<sub>5</sub>O<sub>12</sub> half cell battery gave an initial discharge capacity of  $221 \text{ mAh.g}^{-1}$  which dropped to  $170 \text{ mAh.g}^{-1}$  on the second cycle and stabilized at  $\sim 162 \text{ mAh.g}^{-1}$  for 100 cycles, a value close to the theoretical capacity of  $175 \text{ mAh.g}^{-1}$ . 100% coulombic efficiencies were also observed which indicate minimal energy loss during the charge-discharge cycling process. This electrolyte produced discharge capacity that is 17% more than the conventional electrolyte EC/DMC (1:1) wt/wt, 1 M LiPF<sub>6</sub>. The Li/LiCoO<sub>2</sub> half cell battery gave an initial discharge capacity of  $121 \text{ mAh.g}^{-1}$ , about 88% of the theoretical value. The discharge capacity steadily decreased over cycling losing 36% after 76 cycles which indicate poor reversibility throughout the cycling process. This capacity loss was not observed in the case of the conventional electrolyte EC/DMC (1:1) wt/wt, 1 M LiPF<sub>6</sub> which remained stable at  $128 \text{ mAh.g}^{-1}$ . Similar results were obtained by Sakaebe and Matsumoto<sup>18</sup> who studied Li/LiCoO<sub>2</sub> performance using neat P13-TFSI or PP13 TFSI and LiTFSI as the salt. Cell behavior in case of P13-TFSI/LiTFSI was almost identical to AZ14-TFSI/EC (1:1) wt/wt, 1M LiPF<sub>6</sub> electrolyte with similar initial capacity and capacity loss over cycling. A direct comparison of the battery behavior of electrolytes based on the three ILs (P, PP, AZ) is not possible due to the ability to formulate P-TFSI and PP-TFSI – based electrolytes without the use of an additive or a co-solvent contrary to the case of the AZ-TFSI – based ones.

Li/LiFePO<sub>4</sub> half cell battery was also tested (Figure 6) and gave an initial discharge capacity of  $115 \text{ mAh.g}^{-1}$  which increased gradually to  $127 \text{ mAh.g}^{-1}$  over 90 cycles with efficiencies approaching 94%. This value represents 75% of the theoretical capacity but is comparable with the one obtained using EC/DMC (1:1) wt/wt, 1 M LiPF<sub>6</sub> conventional electrolyte. In the case of both cells, in house synthesized LFP was used which could be the reason for the low initial capacity. In order to investigate this matter, a commercial LFP was later tested and gave initial higher capacity of  $150 \text{ mAh.g}^{-1}$  and  $142 \text{ mAh.g}^{-1}$  using both conventional and AZ14-TFSI/EC (1:1) wt/wt, 1M LiPF<sub>6</sub> respectively, which correspond to 88% of the theoretical capacity for LFP.

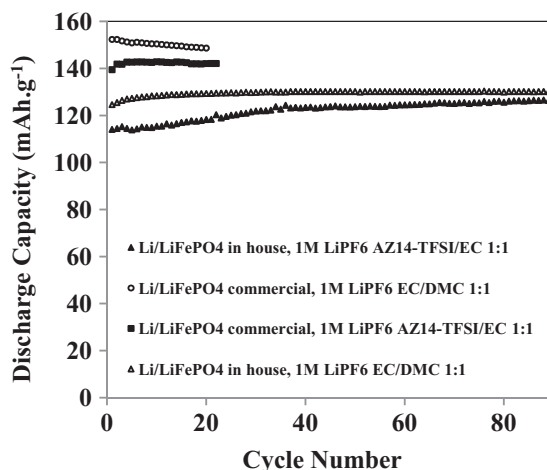


**Figure 6.** Cycling performance of Li/LiFePO<sub>4</sub> half cell batteries.

Li/Graphite half cells were also tested in order to evaluate the Li intercalation and de-intercalation into the graphite anode. Figure 7 shows the charge/discharge curves for the first and second cycles along with the cycling curve over 25 cycles. In the first cycle, the discharge curve shows a plateau in the 0.8–0.2 V range usually indicative of SEI formation mostly from EC decomposition along with other electrolyte components (TFSI reduction) or AZ cation intercalation and another plateau in the 0.2–0 V range that is related to Li<sup>+</sup> intercalation into graphite. The latter can only be observed in the second discharge curve indicating successful SEI formation during the first cycle. Figure 7 also shows that graphite has an initial irreversible capacity of 58 mAh.g<sup>-1</sup> and a discharge capacity of 308 mAh.g<sup>-1</sup> that is fading slightly over

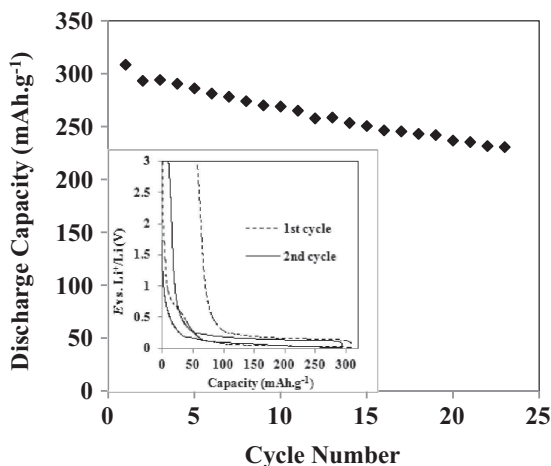


**Figure 7.** Cycling performance of MCMB/Li half cell batteries. Onset: voltage-capacity curve of the first 2 cycles.

cycling reaching 231 mAh.g<sup>-1</sup> at cycle 22. The coulombic efficiency is 99%.

## Conclusions

Ionic liquids based on a new family of imide salts of the ringed ammonium cation Azepanium were synthesized, characterized and tested in lithium batteries. It was found that variation in the molecular structure of the cation gave three room temperature ionic liquids out of the nine salts synthesized. The highly-asymmetric ionic liquids were highly viscous and showed good conductivities. The electrochemical study of the liquids showed low cathodic stability but a wide electrochemical window over 6 volts. The use of ethylene carbonate as a co-solvent led to enhancement in the physical and electrochemical properties of the formulated electrolytes. An electrolyte based on the ionic liquid with the best thermal and electrochemical properties, AZ14-TFSI, and the co-solvent was successfully used to cycle Li/Li<sub>4</sub>Ti<sub>5</sub>O<sub>12</sub> and Li/LiFePO<sub>4</sub> half cell batteries gave high and stable discharge capacities and good coulombic efficiencies, and showed promising capacities in Li/LiCoO<sub>2</sub>.

## References

1. J. Arai, T. Yamaki, S. Yamauchi, T. Yuasa, T. Maeshima, T. Sakai, M. Koseki, and T. Horiba, *Journal of Power Sources*, **146**, 788 (2005).
2. O. Bitsche and G. Gutmann, *Journal of Power Sources*, **127**, 8 (2004).
3. Y. S. Jung, A. S. Cavanagh, A. C. Dillon, M. D. Groner, S. M. George, and S. H. Lee, *Journal of the Electrochemical Society*, **157**, A75 (2010).
4. S. Menkin, D. Golodnitsky, and E. Peled, *Electrochemistry Communications*, **11**, 1789 (2009).
5. S. V. Sazhin, M. K. Harrup, and K. L. Gering, *Journal of Power Sources*, **196**, 3433 (2011).
6. J. Hassoun, A. Fericola, M. A. Navarra, S. Panero, and B. Scrosati, *Journal of Power Sources*, **195**, 574 (2010).
7. V. Borgel, E. Markevich, D. Aurbach, G. Semrau, and M. Schmidt, *Journal of Power Sources*, **189**, 331 (2009).
8. M. Galinski, A. Lewandowski, and I. Stepniak, *Electrochimica Acta*, **51**, 5567 (2006).
9. J. Mun, Y. S. Jung, T. Yim, H. Y. Lee, H.-J. Kim, Y. G. Kim, and S. M. Oh, *Journal of Power Sources*, **194**, 1068 (2009).
10. J. Mun, S. Kim, T. Yim, J. H. Ryu, Y. G. Kim, and S. M. Oh, *Journal of the Electrochemical Society*, **157**, A136 (2010).
11. J. Mun, T. Yim, C. Y. Choi, J. H. Ryu, Y. G. Kim, and S. M. Oh, *Electrochemical and Solid-State Letters*, **13**, A109 (2010).
12. L. Zhao, J.-i. Yamaki, and M. Egashira, *Journal of Power Sources*, **174**, 352 (2007).
13. Y. Abu-Lebdeh, E. Austin, and I. J. Davidson, *Chemistry Letters*, **38**, 782 (2009).
14. S. Fang, Z. Zhang, Y. Jin, L. Yang, S.-i. Hirano, K. Tachibana, and S. Katayama, *Journal of Power Sources*, **196**, 5637 (2011).
15. M. Montanino, M. Carewska, F. Alessandrini, S. Passerini, and G. B. Appetecchi, *Electrochimica Acta*, In Press, Corrected Proof.
16. I. A. Profatilo, N.-S. Choi, S. W. Roh, and S. S. Kim, *Journal of Power Sources*, **192**, 636 (2009).
17. J. H. Shin, P. Basak, J. B. Kerr, and E. J. Cairns, *Electrochimica Acta*, **54**, 410 (2008).
18. H. Sakaebe and H. Matsumoto, *Electrochemistry Communications*, **5**, 594 (2003).
19. P. C. Howlett, D. R. MacFarlane, and A. F. Hollenkamp, *Electrochemical and Solid-State Letters*, **7**, A97 (2004).
20. T. Belhocine, S. A. Forsyth, H. Q. N. Gunaratne, M. Nieuwenhuyzen, A. V. Puga, K. R. Seddon, G. Srinivasan, and K. Whiston, *Green Chemistry*, **13**, 59 (2011).
21. U. p. a. 20080296531.
22. S. Passerini and W. A. Henderson, in *Encyclopedia of Electrochemical Power Sources*, p. 85, Elsevier, Amsterdam (2009).
23. S. P. Ong, O. Andreussi, Y. Wu, N. Marzari, and G. Ceder, *Chemistry of Materials*, **23**, 2979 (2011).
24. K. Xu and A. von Cresce, *Journal of Materials Chemistry*, **21**, 9849 (2011).